# Locating periodic orbits by Topological Degree theory


**C.Polymilis[1], G. Servizi[2], Ch. Skokos[*3,4], G. Turchetti[2] and M.N. Vrahatis[5]**

[1]Department of Physics, University of Athens, Panepistimiopolis, GR-15784, Zografos, Athens, Greece
[2]Department of Physics, Bologna University, Via Irnerio 46, I-40126 Bologna, Italy and I.N.F.N. Sezione di Bologna, Via Irnerio 46, I-40126 Bologna, Italy
[3]Department of Mathematics, Division of Applied Mathematics and Center of Research and Applications of Nonlinear Systems (CRANS), University of Patras, GR-26500, Patras, Greece
[4]Research Center for Astronomy, Academy of Athens, 14 Anagnostopoulou str. , GR-10673, Athens, Greece
[5]Department of Mathematics, University of Patras, GR-26110 Patras, Greece and University of Patras Artificial Intelligence Research Center (UPAIRC), University of Patras, GR-26110 Patras, Greece



## ABSTRACT

We consider methods based on the topological degree theory to compute periodic orbits of area preserving maps. Numerical approximations to the Kronecker integral give the number of fixed points of the map provided that the integration step is small "enough". Since in any neighborhood of a fixed point the map gets four different combination of its algebraic signs we use points on a lattice to detect the candidate fixed points by selecting boxes whose corners show all combinations of sign. This method and the Kronecker integral can be applied to bounded continuous maps such as the beam-beam map. On the other hand they can not be applied to maps defined on the torus, such as the standard map which has discontinuity curves propagating by iteration, or unbounded maps such as the Hénon map. However, the systematic use of the bisection method initialized on the lattice, even though unable to detect all fixed points of a given order, allows us to find a sufficient number of them to provide a clear picture of the dynamics, even for maps on the torus because the discontinuity curves have measure zero.



[*] **e-mail: hskokos@cc.uoa.gr**

## 1. The topological degree (TD) and its computation

We consider the problem of finding the solutions of a system of nonlinear equations of the form $F_n(x) = \Theta_n$, where $F_n = (f_1, f_2, \dots, f_n)$: $D_n \subset \mathbb{R}^n \to \mathbb{R}^n$ is a function from a domain $D_n$ into $\mathbb{R}^n$, $\Theta_n = (0, 0, \dots, 0)^T$ and $x = (x_1, x_2, \dots, x_n)^T$. The above system is equivalent to

$$
\begin{aligned}
f_1(x_1, x_2, \dots, x_n) &= 0,\\
f_2(x_1, x_2, \dots, x_n) &= 0,\\
\\
f_n(x_1, x_2, \dots, x_n) &= 0.
\end{aligned}
$$

The topological degree (TD) theory gives us information on the existence of solutions of the above system, their number and their nature. **Kronecker introduced the concept of the TD in 1869,** while **Picard in 1892 succeeded in providing a theorem for computing the exact number of solutions.** For details about the TD theory and its applications we refer the reader to the following papers and books: Cronin (1964), Lloyd (1978), Vrahatis (1989, 1995), Vrahatis et al. (1996, 1997) and Mourrain et al. (2002).

**Definition.** Consider the function

$$F_n = (f_1, f_2, \dots, f_n) : \overline{D_n} \subset \mathbb{R}^n \to \mathbb{R}^n,$$

which is continuous on the closure $\overline{D_n}$ of $D_n$, such that $F_n(x) \neq \Theta_n$ for x on the boundary $b(D_n)$ of $D_n$. We also consider the solutions of equation $F_n(x) = \Theta_n$ (where $\Theta_n = (0, 0, \dots, 0)^T$), to be simple i.e. the determinant of the corresponding Jacobian matrix ($J_{Fn}$) to be different from zero. Then the ***topological degree of $F_n$ at $\Theta_n$ relative to $D_n$*** is defined as:

$$\boxed{\deg[F_n, D_n, \Theta_n] = \sum_{x \in F_n^{-1}(\Theta_n)} \operatorname{sgn}(\det J_{Fn}(x)) = N_+ - N_-} \qquad (1)$$

where $\det J_{Fn}$ is the determinant of the Jacobian matrix of $F_n$, sgn is the well-known sign function, $N_+$ the number of roots with $\det J_{Fn}>0$ and $N_-$ the number of roots with $\det J_{Fn}<0$.

It is evident that if a nonzero value of deg[$F_n$, $D_n$, $\Theta_n$] is obtained then there exist at least one solution of system $F_n(x) = \Theta_n$ within $D_n$ **(Kronecker's existence theorem).**

## Kronecker's integral

Under the assumptions of the above definition the deg[$F_n$, $D_n$, $\Theta_n$] can be computed by:

deg[$F_n$, $D_n$, $\Theta_n$] =

$$\frac{\Gamma(\frac{n}{2})}{2\,\pi^{n/2}} \iint_{b(D_n)} \cdots \int \frac{\sum_{i=1}^{n} A_i dx_i \cdots dx_{i-1} dx_{i+1} \cdots dx_n}{(f_1^2 + f_2^2 + \cdots + f_n^2)^{n/2}}$$

where

$$A_i = (-1)^{n(i-1)} \begin{vmatrix} f_1 & \frac{\partial f_1}{\partial x_1} & \cdots & \frac{\partial f_1}{\partial x_{i-1}} & \frac{\partial f_1}{\partial x_{i+1}} & \cdots & \frac{\partial f_1}{\partial x_n} \\ f_2 & \frac{\partial f_2}{\partial x_1} & \cdots & \frac{\partial f_2}{\partial x_{i-1}} & \frac{\partial f_2}{\partial x_{i+1}} & \cdots & \frac{\partial f_2}{\partial x_n} \\ \vdots & \vdots & & \vdots & \vdots & & \vdots \\ f_n & \frac{\partial f_n}{\partial x_1} & \cdots & \frac{\partial f_n}{\partial x_{i-1}} & \frac{\partial f_n}{\partial x_{i+1}} & \cdots & \frac{\partial f_n}{\partial x_n} \end{vmatrix}$$

and $\Gamma(x)$ is the gamma function.

## Picard's theorem

We consider the assumptions of the definition of TD. We also consider the function

$$F_{n+1} = (f_1, f_2, \ldots, f_n, f_{n+1}) : D_{n+1} \subset \mathbb{R}^{n+1} \to \mathbb{R}^{n+1}$$

where

$$f_{n+1} = y \, \det J_{F_n},$$

$\mathbb{R}^{n+1}$:$x_1, x_2, \ldots, x_n, y$ and $D_{n+1}$ is the product of $D_n$ with a real interval on the y-axis containing y=0. Then **the exact number N of the solutions** of equation $F_n(x) = \Theta_n$ is

$$N = \deg[F_{n+1}, D_{n+1}, \Theta_{n+1}].$$

## Number of roots for a system of 2 equations

By applying Picard's theorem and Kronecker's in the case of a set of two equations:

$$\begin{aligned} f_1(x_1, x_2) &= 0, \\ f_2(x_1, x_2) &= 0, \end{aligned} \tag{2}$$

we find that **the number N of roots in the domain $D_2 = [a,b]\times[c,d]$ is given by:**

$$\boxed{N = \frac{1}{2\pi} \int_{b(D_2)} (P_1 \, dx_1 + P_2 \, dx_2) + \frac{\varepsilon}{2\pi} \iint_{D_2} \frac{Q \, dx_1 \, dx_2}{(f_1^2 + f_2^2 + \varepsilon^2 J^2)^{3/2}}} \tag{3}$$

where ε an arbitrary positive value, and

$$P_i = \frac{\left( f_1 \frac{\partial f_2}{\partial x_i} - f_2 \frac{\partial f_1}{\partial x_i} \right) \varepsilon J}{(f_1^2 + f_2^2)(f_1^2 + f_2^2 + \varepsilon^2 J^2)^{1/2}}, \quad i = 1,2 \qquad Q = \begin{vmatrix} f_1 & \frac{\partial f_1}{\partial x_1} & \frac{\partial f_1}{\partial x_2} \\ f_2 & \frac{\partial f_2}{\partial x_1} & \frac{\partial f_2}{\partial x_2} \\ J & \frac{\partial J}{\partial x_1} & \frac{\partial J}{\partial x_2} \end{vmatrix}.$$

where J denotes the determinant of the Jacobian matrix of $F_2=(f_1,f_2)$

**Stenger's method** (Stenger 1975).
Stenger's theorem allows us to compute the TD of $F_n$ at a domain $D_n$ if we know the signs of functions $f_1, f_2, \ldots, f_n$ in a 'sufficient' set of points on the boundary $b(D_n)$ of $D_n$.

## 2. The characteristic bisection method

The characteristic bisection method is based on the **characteristic polyhedron** concept for the computation of roots of the equation $F_n(x) = \Theta_n$. The construction of a suitable n-polyhedron, called the characteristic polyhedron, can be done as follows. Let $M_n$ be the $2^n$ n matrix whose rows are formed by all possible combinations of -1 and 1. Consider now an oriented n-polyhedron $\Pi^n$, with vertices $V_k$, k=1,...,2n. If the $2^n$ n matrix of signs associated with F and $\Pi^n$, whose entries are the vectors

$$\mathrm{sgn}F_n(V_k) = (\mathrm{sgn}f_1(V_k), \mathrm{sgn}f_2(V_k), \ldots, \mathrm{sgn}f_n(V_k)), \tag{4}$$

is identical to $M_n$, possibly after some permutations of these rows, then $\Pi^n$ is called the characteristic polyhedron relative to $F_n$. If $F_n$ is continuous, then, after some suitable assumptions on the boundary of $\Pi^n$ we have:

$$\deg[F_n, \Pi^n, \Theta_{n+1}] = \pm 1 \neq 0. \tag{5}$$

So, by applying Kroneker's existence theorem we conclude that there is at least one solution of the system $F_n(x) = \Theta_n$ within $\Pi^n$.

To clarify the characteristic polyhedron concept we consider a function $F_2=(f_1, f_2)$. Each function $f_i$, i=1,2, separates the space into a number of different regions, according to its sign, for some regions $f_i<0$ and for the rest $f_i>0$, i=1,2. Thus, in figure 1(a) we distinguish between the regions where $f_1<0$ and $f_2<0$, $f_1<0$ and $f_2>0$, $f_1>0$ and $f_2>0$, $f_1>0$ and $f_2<0$. Clearly, the following combinations of signs are possible: (-,-), (-,+), (+,+) and (+,-). Picking a point, close to the solution, from each region we construct a characteristic polyhedron. In this figure we can perceive a characteristic and a noncharacteristic polyhedron $\Pi^2$. For a polyhedron $\Pi^2$ to be characteristic all the above combinations of signs must appear at its vertices. Based on this criterion, polyhedron ABDC does not qualify as a characteristic polyhedron, whereas AEDC does.

Next, we describe the **characteristic bisection method. This method simply amounts to constructing another refined characteristic polyhedron, by bisecting a known one, say $\Pi^n$, in order to determine the solution with the desired accuracy.** We compute the midpoint M of an one-dimensional edge of $\Pi^n$, e.g. $<V_i,V_j>$. The endpoints of this one-dimensional line segment are vertices of $\Pi^n$, for which the corresponding coordinates of the vectors, sgn $F_n(V_i)$ and sgn $F_n(V_j)$ differ from each other only in one entry. To obtain another characteristic polyhedron $\Pi^n_*$ we compare the sign of $F_n(M)$ with that of $F_n(V_i)$ and $F_n(V_j)$ and substitute M for that vertex for which the signs are identical. Subsequently, we reapply the aforementioned technique to a different edge (for details we refer to Vrahatis 1988a;b, 1995).

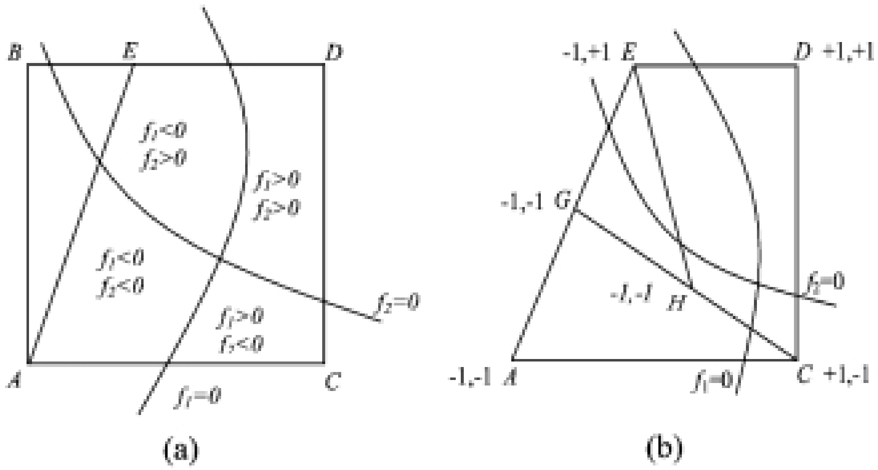


**Figure 1.** (a) The polyhedron ABDC is noncharacteristic while the polyhedron AEDC is characteristic, (b) Application of the characteristic bisection method to the characteristic polyhedron AEDC, giving rise to the polyhedra GEDC and HEDC, which are also characteristic.

**To fully comprehend the characteristic bisection method we illustrate in figure 1(b), its repetitive operation on a characteristic polyhedron $\Pi^2$.** Starting from the edge AE we find its midpoint G and then calculate its vector of signs, which is (-1,-1). Thus, vertex G replaces A and the new refined polyhedron GEDC, is also characteristic. Applying the same procedure, we further refine the polyhedron by considering the midpoint H of GC and checking the vector of signs at this point. In this case, its vector of signs is (-1,-1), so that vertex G can be replaced by vertex H. Consequently, the new refined polyhedron HEDC is also characteristic. This procedure continues up to the point that the midpoint of the longest diagonal of the refined polyhedron approximates the root within a predetermined accuracy.

## 3. Applications

We consider methods based on the topological degree theory to compute periodic orbits of the following area preserving maps:

- **Standard map (map on the torus T)**

$$\mathrm{SM}:\begin{cases} x' = x + y - \dfrac{k}{2\pi}\sin(2\pi x) \\ y' = y - \dfrac{k}{2\pi}\sin(2\pi x) \end{cases} \quad \mathrm{mod}(1), \qquad x, y \in [-0.5, 0.5) \qquad (6)$$

- **Hénon map (unbounded map on $\mathbb{R}^2$)**

$$\mathrm{HM}:\begin{cases} x' = x\cos(2\pi\omega) + (y + x^2)\sin(2\pi\omega) \\ y' = -x\sin(2\pi\omega) + (y + x^2)\cos(2\pi\omega) \end{cases} \qquad (7)$$

- **Beam-beam map (bounded map on $\mathbb{R}^2$)**

$$\mathrm{BM}:\begin{cases} x' = x\cos(2\pi\omega) + (y + 1 - e^{-x^2})\sin(2\pi\omega) \\ y' = -x\sin(2\pi\omega) + (y + 1 - e^{-x^2})\cos(2\pi\omega) \end{cases} \qquad (8)$$

The periodic orbits of the beam-beam map have been studied by Polymilis et al. (1997, 2001).

Given a dynamical map M: $\{x'=g_1(x,y),\ y'=g_2(x,y)\}$, the periodic points of period p are fixed points of $M^p$ and the zeroes of the function:

$$F = M^p - I = \begin{cases} f_1 = g_1^p(x, y) - x \\ f_2 = g_2^p(x, y) - y \end{cases} \qquad (9)$$

where I is the identity matrix.

## Color map

One can use a color map to inspect the geometry of function F (9) and to locate its zeroes. **The color map is created by choosing a lattice of N×N points and by associating to each point a color chosen according to the signs of the functions $f_1$, $f_2$: red for (+,+), green for (+,-), yellow for (-,+), blue for (-,-) as shown in figure 2.** A simple algorithm allows to detect the cells, formed by the lattice of N N points, whose vertices have different colors. A cell is a candidate to have a zero in its interior if the corresponding topological degree is found to be different from zero. In figures 3 and 4 we construct the color map and apply the above mentioned algorithm for locating periodic orbits of period 3 for the SM (6) and of period 5 for the BM (8). The red circles denote the position of the found periodic orbits. We see that for both maps some periodic orbits were not found because some of the four color domains close to the fixed point were very thin. On the other hand, due to the discontinuity of F, some zeros that do not correspond to real periodic orbits were found for the SM (figure 3).

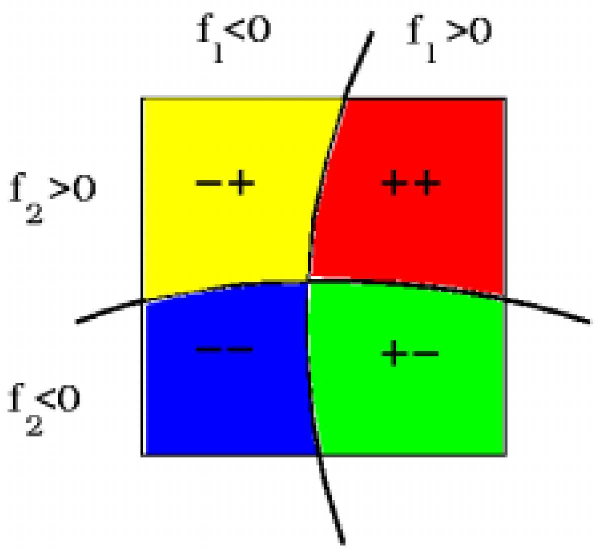


**Figure 2.** Sketch of the domains where functions $f_1$ and $f_2$ (equation 9) have a definite sign.

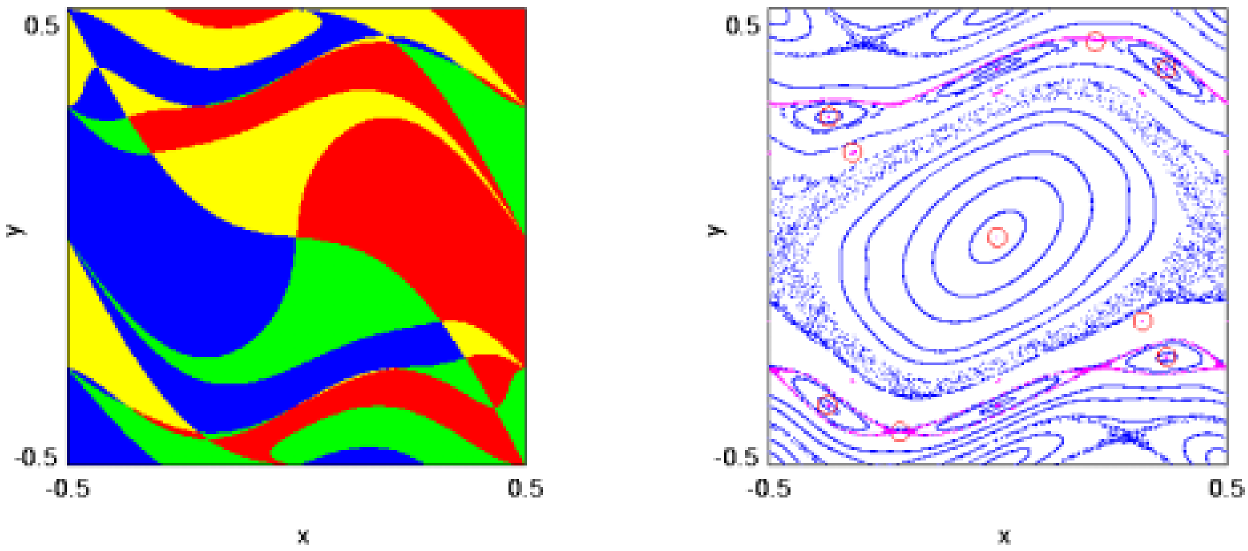


**Figure 3.** Standard map (6) for k=0.9: color map for p=3 iterations of the map computed on a square of N×N points for N=512 (left panel); phase plot of the map (right panel). The red circles denote the position of the zeros of the corresponding function (9).

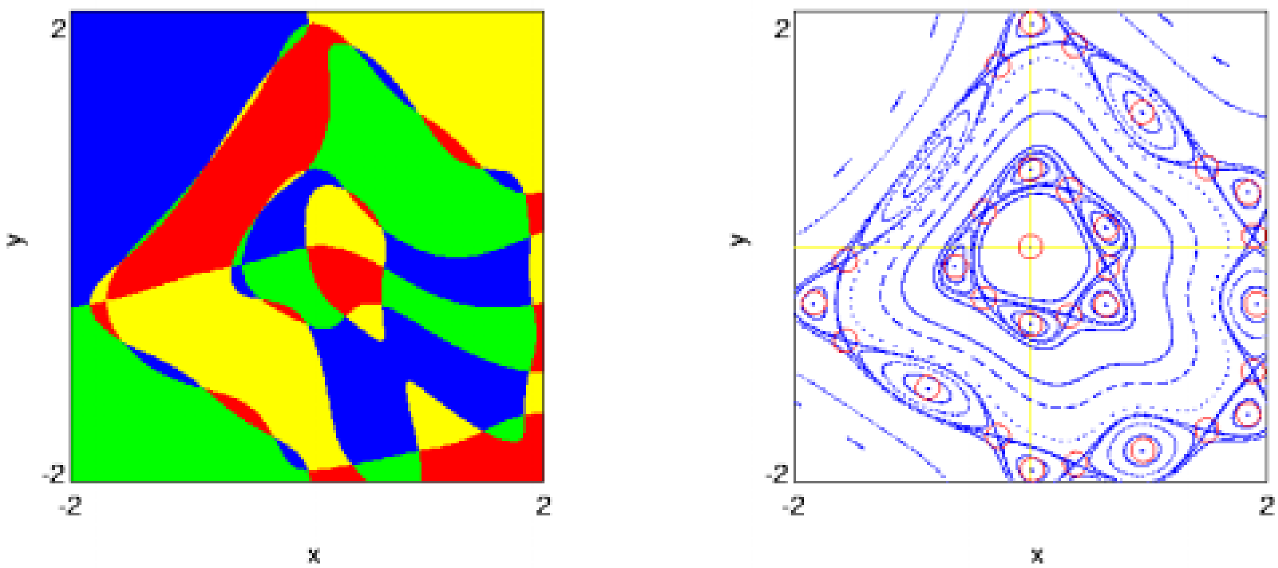


**Figure 4.** Beam-beam map (8) for ω=0.21: color map for p=5 iterations of the map computed on a square of N×N points for N=512 (left panel); phase plot of the map (right panel). The red circles denote the position of the zeros of the corresponding function (9).

## Discontinuity curves

For maps defined on the torus like the SM (6), the computation of the TD using Stenger's method or the Kronecker integral (3) faces a problem due to the presence of discontinuity curves. Indeed the above integral is defined on a domain where F (9) is continuous.

For the SM the discontinuity curves are the lines x=-0.5 and y=-0.5, plotted in red and blue color respectively at the left panel of figure 5. By applying the SM map M once these lines are mapped on the red and blue curves seen in the right panel of figure 5. On the initial phase space there exist also the discontinuity curves that will be mapped after one iteration to the lines x=-0.5 and y=-0.5. These curves are plotted in black and green color respectively in figure 5. These curves can be produced by applying the inverse SM to the discontinuity lines x=-0.5 and y=-0.5. So the discontinuity curves divide the initial phase space in five continuous regions marked as I, II, III, IV and V in figure 5. In each region the computation of the TD can be performed accurately by Stenger's method or by Kronecker's integral evaluation. If, however, **the boundary of the domain where these procedures are applied, cross a discontinuity curve the results we get are not correct (figure 6).**

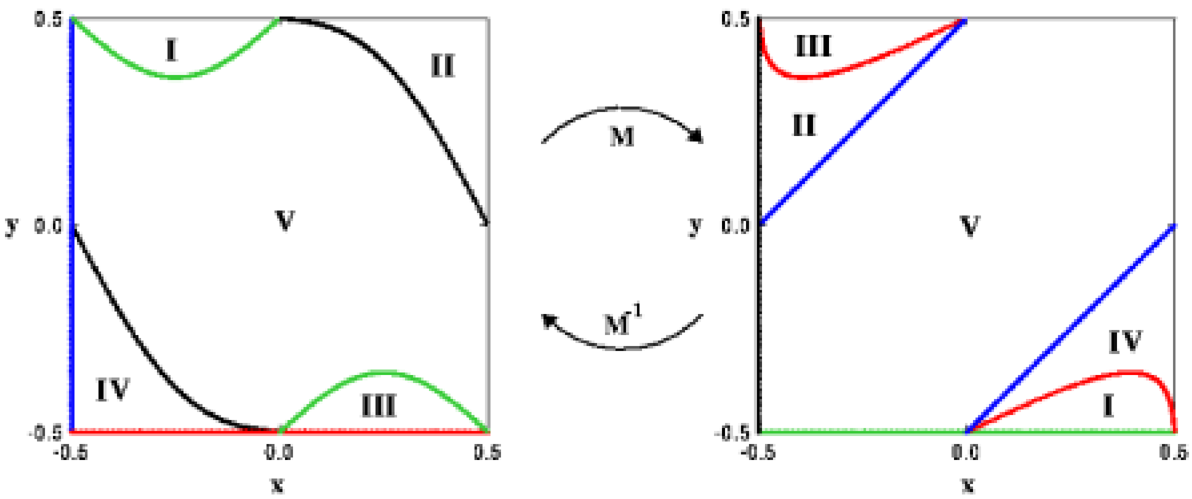


**Figure 5.** The discontinuity curves of the standard map M (6) divide the phase space in five continuous regions (I, II, III, IV, V). In each region the computation of the TD can be performed accurately.

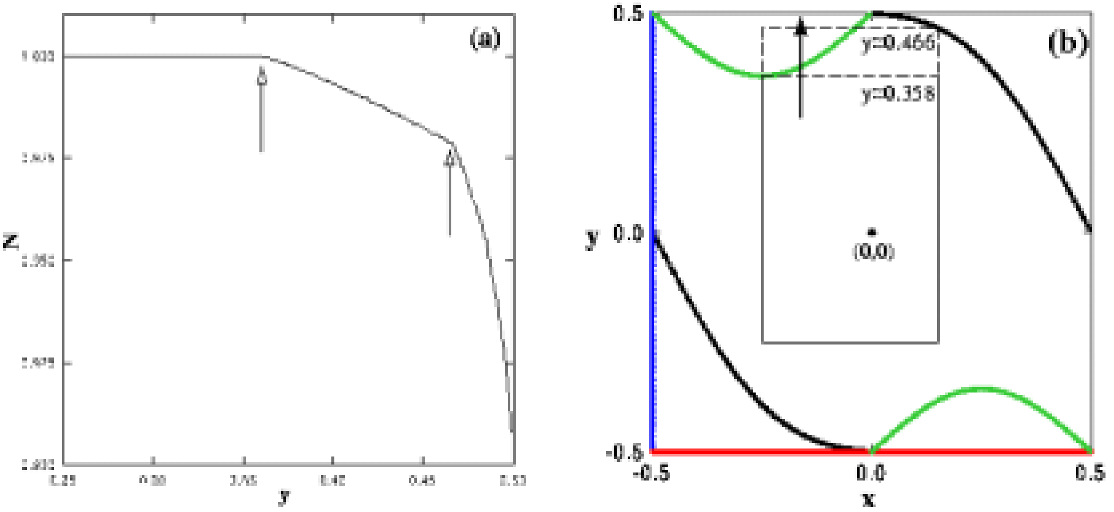


**Figure 6.** (a) Number of fixed points N evaluated for the SM (6) with k=0.9 using the Kronecker's integral (3), in a rectangular domain whose topside moves. The rectangle and the discontinuity lines are shown in (b). For the various rectangles, N should be equal to 1 since they contain only 1 fixed point of period 1, point (0,0). The two points marked by arrows in (a) where N deviates from the correct value N=1, correspond to $y \approx 0.358$ and $y \approx 0.466$ respectively, where the upper-side of the rectangular crosses the two discontinuity curves in (b).

## Roots near the boundary

We consider the simple map $F^*=(f_1,f_2)$ : $f_1(x,y)=y-x^3/3+x$, $f_2(x,y)=y$. The lines $f_1=0$, $f_2=0$ are plotted in figure 7(a). The above system of equations has three roots. The determinant of the corresponding Jacobian matrix ($\det J_{F^*}$) is positive for root (0,0) and negative for roots $(-\sqrt{3},0)$ and $(\sqrt{3},0)$.

In order to **study the dependence of the procedure for finding the TD in a region D, with respect to the distance of a root from the boundary of D,** we consider a rectangular of the form $[-a,2]$ $[-2,2]$ with $a>\sqrt{3}$, shown in the figure 7(a). Since this domain contains the three roots of system the value of TD is -1. We let $a=\sqrt{3}+\varepsilon$ with $\varepsilon>0$ so that the boundary approaches the root as $\varepsilon \to 0$, as shown by the arrow in figure 7(a). We compute the TD for different values of $\varepsilon$ by Stenger's method, by using the same number of points N on every side of the rectangle. We denote by $n_{gp}=4N$ the smallest number of grid points needed to compute the TD with certainty. In figure 6(b) we plot in log-log scale, $n_{gp}$ with respect to $\varepsilon$ (dashed line). The slope of the curve is almost -1 so that $N \propto \varepsilon^{-1}$. The same result holds for any map when a root approaches the boundary (the solid line in figure 7(b) is obtained for a similar example for the SM (6)).

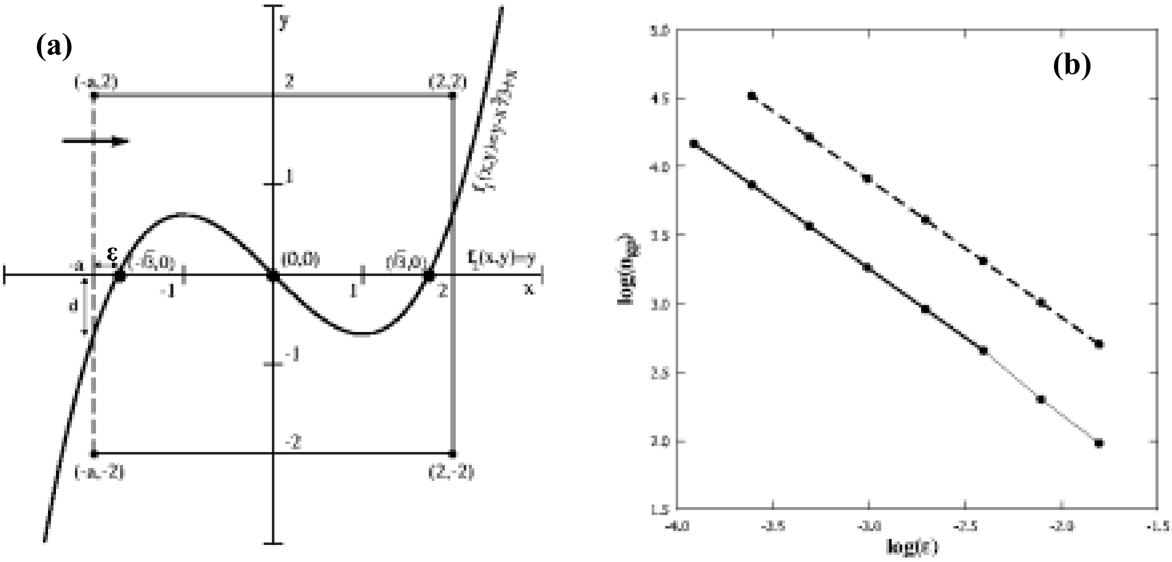

Figure 7. (a) Plot of the curves $f_1 \equiv y - x^3/3 + x = 0$, $f_2 \equiv y = 0$. (b) Dependence of the number of iteration points $n_{gp}$, needed for computing the correct value of the TD in a domain, on the distance ε of a root from the boundary of the domain, for the set of equations of (a) (dashed line) and the SM (continuous line).

## Periodic orbits

Using the characteristic bisection method we were able to **compute a sufficient number of the periodic orbits with period up to 40 for the BM (figure 8) and the SM (figure 9).**

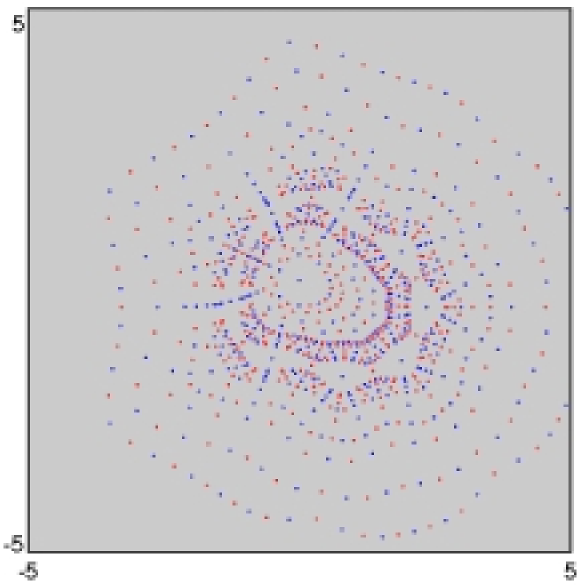


Figure 8. Periodic orbits up to period p=40 for the BM (8) for ω=0.14. The elliptic periodic orbits are blue and the hyperbolic ones are red.

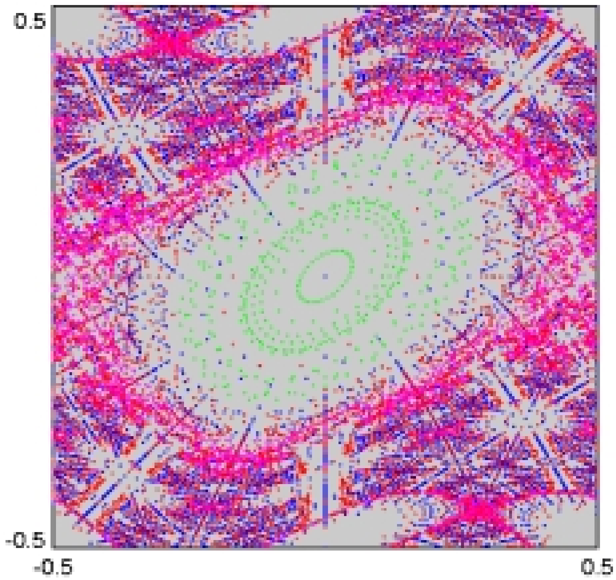


**Figure 8.** Periodic orbits up to period p=40 for the SM (8) for k=0.9. Different colors denote different kind of stability: the elliptic periodic orbits are blue, the hyperbolic periodic orbits are red and the hyperbolic with reflection periodic orbits are pink. The marginally stable periodic orbits, having $| |\det J_F| - 2 | < 10^{-6}$, are green.

## 4. Synopsis

We have studied the applicability of various numerical methods, based on the topological degree theory, for locating high period periodic orbits of 2D area preserving mappings.

In particular we have used the **Kronecker's integral** and applied the **Stenger's method for finding the TD** in a bounded region of the phase space. If the TD has a non-zero value we know that there exist at least one periodic orbit in the corresponding region. The computation of the TD for an appropriate set of equations allows us **to find the exact number of periodic orbits.** We also applied the **characteristic bisection method** on a mesh in the phase space for **locating the various fixed points**.

The main advantage of all these methods is that they are not affected by accuracy problems in computing the exact values of the various functions used, since, the only computable information needed is the algebraic signs of these values.

We have applied the above-mentioned methods to 2D symplectic mappings defined on $R^2$ and on the torus $T^2$. The methods for computing the TD are applied to continuous regions of the phase space, so their use for maps on the torus is limited to regions where no discontinuity curves exist. On the other hand **the characteristic bisection method proved to be very efficient for all different types of mappings, since, it allowed us to compute a big fraction of the real fixed points of period up to 40 in reasonable computational times**. Finally we believe that this method can be extended also to higher dimensional maps.

## References


1. Cronin J. (1964), *Fixed points and topological degree in nonlinear analysis*, Mathematical Surveys No. 11, Amer. Math. Soc., Providence, Rhode Island.
2. Lloyd N. G. (1978), *Degree Theory*, Cambridge University Press, Cambridge.
3. Mourrain B., Vrahatis M. N. & Yakoubsohn J. C. (2002), J. Complexity, 18, 612.
4. Polymilis C., Servizi G. & Skokos Ch. (1997), Cel. Mech. Dyn. Astron., 66, 365.
5. Polymilis C., Skokos Ch., Kollias G., Servizi G. & Turchetti G. (2000), J. Phys. A, 33, 1055.
6. Stenger F. (1975), Numer. Math., 25, 23.
7. Vrahatis M.N. (1988a), ACM Trans. Math. Software, 14, 312.
8. Vrahatis M.N. (1988b), ACM Trans. Math. Software, 14, 330.
9. Vrahatis M. N. (1989), Proc. Amer. Math. Soc., 107, 701.
10. Vrahatis M. N. (1995), J. Comp. Phys., 119, 105.
11. Vrahatis M. N., Bountis T. C. & Kollmann M. (1996), Inter. J. Bifurc. Chaos, 6, 1425.
12. Vrahatis M.N., Isliker H. & Bountis T. C. (1997), Inter. J. Bifurc. Chaos, 7, 2707.